

# ORA waveform-derived biomechanical parameters to distinguish normal from keratoconic eyes

## Parâmetros biomecânicos derivados da forma da curva do ORA para discriminar olhos normais de ceratocones

ALLAN LUZ<sup>1,2,3</sup>, BRUNO MACHADO FONTES<sup>1,3</sup>, BERNARDO LOPES<sup>3</sup>, ISAAC RAMOS<sup>3</sup>, PAULO SCHOR<sup>1</sup>, RENATO AMBRÓSIO JR.<sup>1,3,4</sup>

### ABSTRACT

**Purpose:** To evaluate the ability of the Ocular Response Analyzer (ORA; Reichert Ophthalmic Instruments, Buffalo, NY) to distinguish between normal and keratoconic eyes, by comparing pressure and waveform signal-derived parameters.

**Methods:** This retrospective comparative case series study included 112 patients with normal corneas and 41 patients with bilateral keratoconic eyes. One eye from each subject was randomly selected for analysis. Keratoconus diagnosis was based on clinical examinations, including Placido disk-based corneal topography and rotating Scheimpflug corneal tomography. Data from the ORA best waveform score (WS) measurements were extracted using ORA software. Corneal hysteresis (CH), corneal resistance factor (CRF), Goldman-correlated intraocular pressure (IOPg), cornea-compensated intraocular pressure (IOPcc), and 37 parameters derived from the waveform signal were analyzed. Differences in the distributions among the groups were assessed using the Mann-Whitney test. Receiver operating characteristic (ROC) curves were calculated.

**Results:** Statistically significant differences between keratoconic and normal eyes were found in all parameters ( $p < 0.05$ ) except IOPcc and W1. The area under the ROC curve (AUROC) was greater than 0.85 for 11 parameters, including CH (0.852) and CRF (0.895). The parameters related to the area under the waveform peak during the second and first applanations (p2area and p1area) had the best performances, with AUROCs of 0.939 and 0.929, respectively. The AUROCs for CRF, p2area, and p1area were significantly greater than that for CH.

**Conclusion:** There are significant differences in biomechanical metrics between normal and keratoconic eyes. Compared with the pressure-derived parameters, corneal hysteresis and corneal resistance factor, novel waveform-derived ORA parameters provide better identification of keratoconus.

**Keywords:** Cornea; Keratoconus; Corneal diseases; Refractive surgical procedures; Software; Biomechanics

### RESUMO

**Objetivo:** Avaliar a capacidade do Ocular Response Analyzer (ORA; Reichert Ophthalmic Instruments, Buffalo, NY) em discriminar olhos com ceratocone de olhos normais e comparar parâmetros derivados da pressão dos parâmetros derivados da forma da curva.

**Métodos:** Estudo comparativo retrospectivo série de casos que incluiu 112 pacientes com olhos normais e 41 pacientes com ceratocone bilateral. Um olho de cada indivíduo foi randomicamente selecionado para análise. O diagnóstico de ceratocone foi baseado em exame clínico, incluindo topografia de Plácido e tomografia Scheimpflug. Informação do melhor waveform score foi extraída do software do ORA. Histerese corneana (CH), fator de resistência corneana (CRF), pressão intraocular correlacionada com Goldman (IOPg), pressão intraocular compensada pela córnea (IOPcc) e 37 novos parâmetros derivados da forma da curva do sinal do ORA foram analisados. Diferenças nas distribuições dos grupos foram avaliadas pelo teste Mann-Whitney. Curvas ROC foram calculadas.

**Resultados:** Diferenças estatisticamente significantes foram encontradas entre os olhos normais e ceratocones em todos os parâmetros ( $p < 0,05$ ) salvo IOPcc e W1. A área sob a curva ROC (AUROC) foi maior que 0,85 em 11 parâmetros, incluindo CH (0,852) a CRF (0,895). Os parâmetros relacionados com a área sob o pico da forma de onda durante a segunda e primeira applanção (p2area e p1area) obtiveram as melhores performances, com AUROCs de 0,939 e 0,929, respectivamente. Os valores de AUROCs do fator de resistência corneana, p2area e p1area foram significativamente maiores que os valores de histerese corneana. **Conclusão:** Existem diferenças significantes nas medidas biomecânicas entre olhos normais e com ceratocone. Comparados com os parâmetros derivados da pressão, histerese corneana e fator de resistência corneana, os parâmetros derivados da forma da curva proporcionaram melhor identificação dos ceratocones.

**Descritores:** Córnea; Ceratocone; Doenças da córnea; Procedimentos cirúrgicos refrativos; Software; Biomecânica

### INTRODUCTION

In 2005, the Ocular Response Analyzer (ORA; Reichert Technologies, Depew, New York) was launched as the first commercial device claiming to provide *in vivo* measurements of corneal biomechanics<sup>(1)</sup>. It utilizes a dynamic bi-directional applanation process in which two applanation pressure measurements are recorded: the first, while the cornea is moving inward (P1); and the second, while the cornea returns<sup>(2)</sup>.

The primary output measurements, derived from the air puff recorded pressure during the first and second applanations, are

Goldmann-correlated intraocular pressure (IOPg), defined as the average between P1 and P2; corneal hysteresis (CH), defined as the difference between P1 and P2; corneal resistance factor (CRF), which includes a constant factor designed to optimize the correlation with central corneal thickness (CCT); and corneal compensated intraocular pressure (IOPcc), which includes a constant based on CRF for correlation with CCT<sup>(2)</sup>.

Further information about the corneal response is provided by infrared waveform signal analysis, which corresponds to the deformation movement of the cornea caused by the air puff<sup>(3)</sup>. These novel

Submitted for publication: April 9, 2012  
Accepted for publication: January 31, 2013

Study carried out at Instituto de Olhos Renato Ambrósio - Rio de Janeiro, Brazil.

<sup>1</sup> Department for Ophthalmology of the Universidade Federal de São Paulo, São Paulo, Brazil.

<sup>2</sup> Hospital de Olhos de Sergipe, Aracaju, Brazil.

<sup>3</sup> Rio de Janeiro Corneal Tomography and Biomechanics Study Group.

<sup>4</sup> Instituto de Olhos Renato Ambrósio, Visare Personal Laser and Refracta-RIO, Rio de Janeiro, Brazil.

**Funding:** No specific financial support was available for this study.

**Disclosure of potential conflicts of interest:** A.Luz, None; B.M.Fontes, None; B.Lopes, None; I.Ramos, None; P.Schor, None, R.Ambrósio Jr, is a consult of OCULUS Optikgeräte GmbH.

**Correspondence address:** Allan Luz. Rua Campo do Brito, 995 - Aracaju (SE) - 49020-380 - Brazil - E-mail: allanluz@uol.com.br

The ethics committee of the Universidade Federal de São Paulo, Brazil (protocol 1210/10).

parameters based on a complex analysis of the waveform signal were thought to improve sensitivity and specificity for distinguishing normal and keratoconic corneas<sup>(2-5)</sup>.

Kerautret et al., reported a case that demonstrated the importance of ORA waveform signal analysis in the evaluation of LASIK-induced ectasia compared with a stable post-LASIK cornea with a similar CH value<sup>(6)</sup>.

Parameters from the waveform signal have been studied for staging the severity of keratoconus<sup>(7)</sup>. In addition, changes after myopic LASIK and the estimated elasticity coefficient of the cornea were evaluated using waveform signal parameters<sup>(8,9)</sup>. Although CH and CRF were found to be unchanged after corneal crosslinking (CXL)<sup>(10,11)</sup>, waveform-derived parameters were significantly changed after CXL<sup>(3,12)</sup>.

In a previous study<sup>(13)</sup>, our group reported lower values for keratoconic eyes with normal central corneal thickness. Many other studies by different investigators have also found lower values for keratoconus<sup>(14-16)</sup>, by testing only the traditional ocular biomechanical metrics pressure-derived parameters CH and CRF.

This study was conducted to evaluate pressure-derived parameters (CH, CRF, IOPg, and IOPcc) and 37 novel parameters derived from the waveform signal of the ORA with regard to their ability to distinguish normal from keratoconic eyes.

**METHODS**

The study constituted a comparative case series. The retrospective study involved 112 patients with normal corneas and 41 patients with bilateral keratoconus; one eye from each subject was randomly selected. The research followed the tenets of the Declaration of Helsinki and was approved by the ethics committee of the Federal University of São Paulo, Brazil (protocol 1210/10).

Patients examined at the Instituto de Olhos Renato Ambrósio (Rio de Janeiro, Brazil) were retrospectively enrolled. Patients were selected from a database of patients with normal corneas who were candidates for refractive surgery and from a database of cases diagnosed as having keratoconus in both eyes.

All eyes were examined by a fellowship-trained cornea and refractive surgeon (R.A.). Along with a comprehensive ocular examination, all eyes were examined by Placido disk-based corneal topography (Atlas Corneal Topography System; Humphrey, San Leandro, CA) and rotating Scheimpflug corneal tomography (Pentacam HR; Oculus, Wetzlar, Germany). The diagnosis of keratoconus was made based on clinical data, including Placido disk-based axial topography corneal curvature maps<sup>(17)</sup>; criteria used in the Collaborative Longitudinal Evaluation of Keratoconus study<sup>(18)</sup>; and Pentacam corneal tomography<sup>(5)</sup>. Keratoconus cases with a history of corneal surgery or with extensive corneal scarring were excluded from the study.

The patients underwent clinical evaluation and testing with the ORA during the same visit. All measurements were obtained between 8 AM and 6 PM. At least two consecutive measurements were performed, and the best waveform score (WS) from each patient was included in the analysis.

The ORA determines corneal biomechanical properties by using an applied force displacement relationship, as described previously<sup>(1,14-16)</sup>. Briefly, a precisely metered air pulse is delivered to the eye, causing the cornea to move inward, past applanation, and into slight concavity. Milliseconds after the initial applanation, the air pump generating the air pulse is shut off, and the pressure applied to the eye decreases in an inverse-time, symmetrical fashion. As the pressure decreases, the cornea passes through a second applanated state while returning from concavity to its normal convex curvature. Energy absorption during rapid corneal deformation delays the occurrence of the inward and outward applanation signal peaks, resulting in a difference between the applanation pressures. The difference between these inward and outward motion applanation pressures is

the CH, which indicates viscous damping in the cornea and reflects the capacity of corneal tissue to absorb and dissipate energy. CRF is a measure of the cumulative effects of both the viscous and elastic resistance encountered by the air jet while deforming the corneal surface; it is an indicator of the overall resistance of the cornea. The CRF was derived empirically to maximize its correlation with the central corneal thickness<sup>(19)</sup>. It can be considered as weighted by the elastic resistance, because of its stronger correlation with the central corneal thickness than with CH. Although CH and CRF are related, they can differ significantly in some cases, and each provides distinct information about the cornea.

Using the new ORA software (version 2.04), the 37 new parameters described in table 1 were calculated based on the waveform of the ORA signal. Statistical analyses were performed using BioEstat 5.0 (Instituto Mamirauá, Amazonas, Brazil) and Med-Calc 11.1 (MedCalc Software, Mariakerke, Belgium). The nonparametric Mann-Whitney *U* test (Wilcoxon rank sum test) was used to assess variable distributions between the keratoconic and normal cornea groups.

Receiver operating characteristic (ROC) curves and the areas under the ROC curves (AUROCs) were calculated for all parameters to determine the test's overall predictive accuracy. The standard error of the AUROC was assessed with the DeLong method<sup>(20)</sup>. The binomial exact method was used to calculate the confidence interval (CI) for the AUROC. Nonparametric pairwise comparisons were performed to determine the significance of differences between AUROCs, using the Hanley-McNeil method for calculating the standard error<sup>(21)</sup>. Values of *P*<0.05 indicated statistical significance.

**RESULTS**

Single eyes randomly selected from the 112 patients with normal unoperated eyes and 41 patients with bilateral keratoconus were enrolled. In the normal and keratoconic groups, the average patient ages were 39.0 ± 17.9 years (range: 12.0 to 78.1 years) and 30.2 ± 10.8 years (range: 16.1 to 63 years), respectively, and the male/female percentages were 40.1/59.9 and 63.3/36.4, respectively.

The SimK1 and SimK2 simulated keratometry values and the maximal keratometry value in the keratoconic group were 47.52 ± 5.53 diopters (D) (range: 39.90 to 69.40 D), 49.75 ± 7.12 D (range: 41.80 to 72.80), and 55.59 ± 7.63 D (range: 45.38 to 83.19 D), respectively.

Significant differences were found between normal and keratoconic eyes for all parameters (Mann-Whitney *U* test, *P*<0.05) with the

**Table 1. Designation of the parameters**

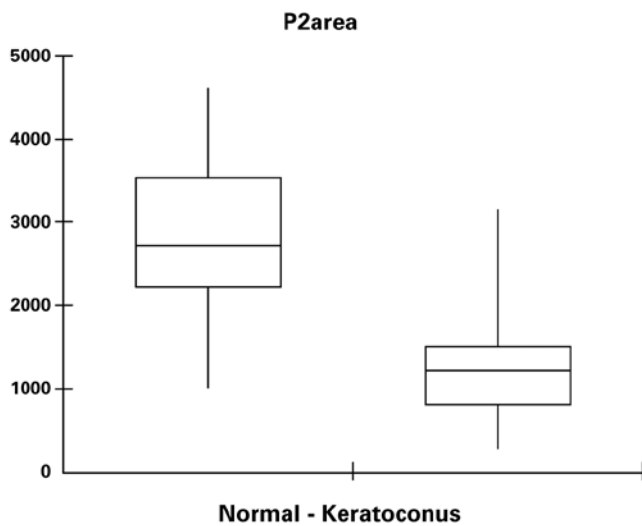
Parameter	Upper 75% of peak height (23 parameters)	Upper 50% of peak height (14 parameters)
Area	p1area, p2area	p1area1, p2area1
Height	h1, h2	h11, h21
Width	w1, w2	w11, w21
Aspect ratio	aspect1, aspect2	aspect11, aspect21
Slope	uslope1, dslope1, uslope2, dslope2	uslope11, dslope11, uslope21, dslope21
Slew rate	slew1, slew2, mslew1, mslew2	—
Path	path1, path2	path11, path21
Irregularity	aindex, bindex	—
Dive	dive1, dive2	—
High frequency	aphf	—

1 = first peak of upper 75% of peak height, 2 = second peak of upper 75% of peak height, 11 = first peak of upper 50% of peak height, 21 = second peak of upper 50% of peak height<sup>3</sup>.

**Table 2. ORA parameters measured in normal and keratoconus eyes**

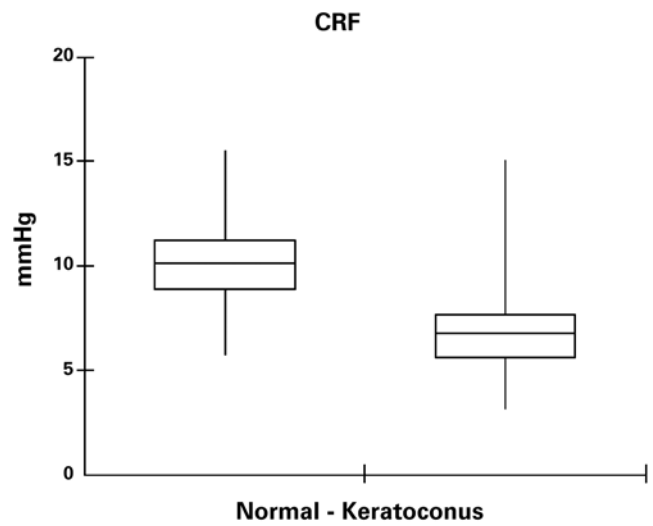
	Normal					Kerato			
	Mean	SD	Max	Min	P value U	Mean	SD	Max	Min
CH	10,34	1,67	14,30	5,50	<0.0001	7,85	1,79	13,40	4,40
CRF	10,08	1,83	15,50	5,70	<0.0001	6,89	2,07	15,00	3,10
IOPg	14,55	3,34	25,60	6,90	<0.0001	10,97	3,54	22,20	4,30
IOPcc	15,23	3,21	26,30	7,60	0.1375	14,82	3,15	26,40	9,50
aindex	9,09	1,22	10,00	3,82	<0.0001	7,21	2,63	10,00	1,25
bindex	9,40	1,05	10,00	4,65	0.0032	7,70	3,02	10,00	0,21
p1area	4371,53	1233,63	9037,44	1402,00	<0.0001	2123,88	1060,98	4849,13	278,19
p2area	2837,73	851,47	4610,50	993,63	<0.0001	1263,50	614,66	3138,88	272,75
aspect1	22,60	6,28	39,31	7,82	<0.0001	13,55	7,71	44,19	2,37
aspect2	23,07	9,62	55,02	4,63	<0.0001	16,89	13,27	66,71	2,80
uslope1	81,36	32,91	187,17	25,81	<0.0001	43,99	29,40	140,75	5,69
uslope2	104,10	44,29	239,13	14,68	<0.0001	57,41	41,39	176,38	6,25
dslope1	32,59	9,29	60,83	11,55	<0.0001	20,84	11,02	60,79	3,83
dslope2	30,52	14,05	83,21	5,59	0.0010	26,56	26,56	146,13	3,08
w1	21,64	2,99	30,00	15,00	0.0514	20,68	5,09	31,00	10,00
w2	18,21	3,86	34,00	10,00	0.0108	16,39	6,74	37,00	5,00
h1	477,40	109,20	644,44	225,00	<0.0001	257,92	110,68	458,06	68,63
h2	392,15	111,84	621,75	156,19	<0.0001	215,36	106,57	545,81	69,95
dive1	398,96	148,23	636,50	17,50	<0.0001	205,84	117,07	439,00	17,50
dive2	319,04	110,55	601,50	120,50	<0.0001	157,20	88,56	382,50	16,25
path1	22,02	3,80	35,64	14,17	<0.0001	28,47	10,22	54,86	14,67
path2	26,08	6,34	51,14	11,57	<0.0001	33,79	9,45	59,00	18,43
mslew1	133,45	42,71	239,50	41,75	<0.0001	77,36	39,51	184,00	20,25
mslew2	154,00	57,95	332,75	34,75	<0.0001	98,24	56,81	255,00	16,25
slew1	81,29	34,63	187,17	17,50	<0.0001	46,41	29,23	140,75	11,29
slew2	104,26	43,99	239,13	23,31	<0.0001	62,38	39,23	176,38	9,50
aplhf	1,34	0,31	2,50	0,90	<0.0001	1,74	0,44	3,10	1,00
p1area1	1891,81	628,60	4362,63	564,25	<0.0001	900,96	510,77	2468,63	117,75
p2area1	1225,07	398,54	2142,25	380,75	<0.0001	536,47	293,80	1556,25	123,50
aspect11	29,81	9,88	66,25	10,71	<0.0001	19,63	12,29	63,84	4,19
aspect21	32,29	14,25	69,91	4,56	<0.0001	22,93	15,84	66,88	3,90
uslope11	78,68	35,25	181,38	18,63	<0.0001	44,12	27,31	128,25	9,75
uslope21	85,60	38,35	198,00	15,13	<0.0001	52,95	41,90	176,38	9,50
dslope11	50,13	22,36	154,13	15,30	<0.0001	36,27	25,69	128,38	5,83
dslope21	50,73	27,27	137,38	5,79	0.0027	40,56	32,01	131,75	5,71
w11	11,18	2,12	17,00	5,00	0.0108	9,88	3,51	17,00	4,00
w21	9,02	2,76	23,00	4,00	0.0003	7,37	2,77	17,00	4,00
h11	318,27	72,80	429,63	150,00	<0.0001	171,94	73,79	305,38	45,75
h21	261,43	74,56	414,50	104,13	<0.0001	143,57	71,05	363,88	46,63
path11	31,70	7,64	57,88	15,19	0.0006	38,59	11,98	69,00	16,70
path21	36,28	9,97	66,57	14,59	0.0002	45,01	13,60	74,37	22,08

Significant differences were found between normal and keratoconic eyes for all parameters (Mann-Whitney U test,  $P < 0.05$ ) with the exception of IOPcc ( $P = 0.1375$ ) and W1 ( $P = 0.0514$ ).



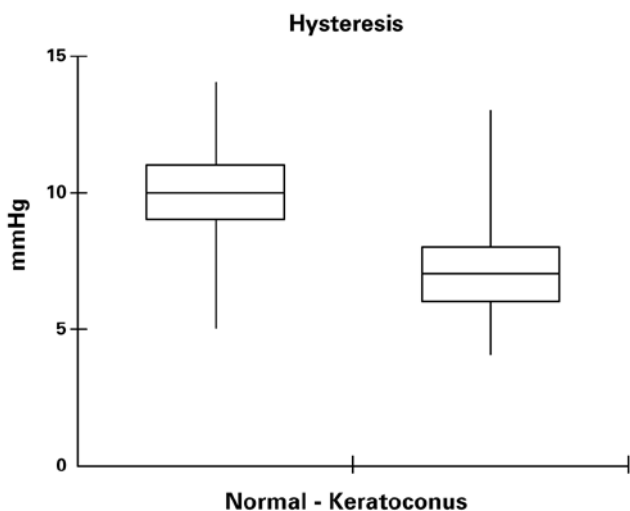
Demonstration of the overlapped values P2area

Figure 1. Distribution of normal and keratoconus eyes for P2area.



Demonstration of the overlapped values CRF

Figure 3. Distribution of normal and keratoconus eyes for CRF.



Demonstration of the overlapped values CH

Figure 2. Distribution of normal and keratoconus eyes for CH.

exception of IOPcc ( $P=0.1375$ ) and W1 ( $P=0.0514$ ) (Table 2). Corneal hysteresis was  $7.85 \pm 1.79$  mmHg (range: 13.40 to 4.40 mmHg) in the keratoconus group and  $10.34 \pm 1.67$  mmHg (range: 14.30 to 5.50) in the control group ( $P<0.0001$ ). The corneal resistance factor was  $6.89 \pm 2.07$  mmHg (range: 15.0 to 3.10) in the keratoconus group and  $10.08 \pm 1.83$  mmHg (range: 15.50 to 5.70) in the control group ( $P<0.0001$ ). The p2area was  $1263.50 \pm 614.66$  (range to 3138.88 to 272.75) in the keratoconus group and  $2837.73 \pm 851.47$  (range: 4610.50 to 993.63) in the control group ( $P<0.0001$ ). The p1area was  $2123.88 \pm 1060.98$  (range: 4849.13 to 278.19) in the keratoconus group and  $4371.53 \pm 1233.63$  (range: 9037.44 to 1402.00 ( $P<0.0001$ )). The data are summarized in table 2. Box-plot distributions of p2area, CH and CRF are shown in figures 1, 2 and 3, respectively.

The AUROC was greater than 0.85 for 11 parameters, including CH (0.852) and CRF (0.895). The parameters related to the area of the waveform during the second and first applanations had the best performances, with AUROCs of 0.939 and 0.929 for p2area and p1area,

respectively (Table 3). The AUROCs for p2area, p1area, and CRF were significantly greater than the AUROC for CH. Table 4 summarizes the pairwise comparisons of ROC curves for the 11 parameters with AUROCs  $>0.85$ .

## DISCUSSION

The identification of keratoconus and related conditions when screening refractive candidates is of particularly high clinical importance because failure to identify these cases is considered to be the main cause of ectasia after LASIK<sup>(5,22,23)</sup>. This study analyzed 37 novel waveform signal parameters using the ORA 2.04 software and demonstrated that the classic CH and CRF pressure parameters might not be used to distinguish normal eyes from those with keratoconus, as significant overlap is present.

The keratoconic cornea has a conical curvature with three characteristic features: thinning of the corneal stroma with folding artifacts, breaks in the Bowman's layer due to a weak collagen fiber network and deposition of iron in the basal layers of the corneal epithelium. Additional structural changes may also be observed depending on the severity of the disease<sup>(24)</sup>. A decrease in the number of collagen lamellae concomitant with an increase in the ground substance (proteoglycans) is frequently observed in the stroma<sup>(25)</sup>. Loss of collagen fibrils in the stroma has been linked to proteolytic enzymes or decreased levels of proteinase inhibitors such as corneal  $\alpha 1$  inhibitor and  $\alpha 2$  macroglobulin<sup>(26)</sup>.

Keratoconic eyes have low tensile strength, thinning, and protrusion<sup>(27)</sup>. Lower resistance to deformation is attributable not only to thinning but also to the presence of more fragile corneal stromal collagen fibrils in keratoconic eyes than in normal eyes<sup>(13)</sup>. Thus, reduced central corneal thickness is only part of the screening process for keratoconus identification. Previous studies<sup>(22,28)</sup> have demonstrated that biomechanical pressure metrics are significantly lower in keratoconus corneas than in normal corneas.

Data presented by Fry and David Luce<sup>(7)</sup> suggested that waveform parameters provided from the ORA signal may be more sensitive than the pressure parameters CH and CRF in identifying abnormal corneas. CH and CRF had different distributions between normal and keratoconic corneas in the present study. Nevertheless, significant overlap was noted and even for the new parameters in the present study, no cutoff value with high sensitivity and specificity could be established for the differentiation of keratoconus and

**Table 3. Data summary from receiver operating characteristic curve of new ora parameters in normal and keratoconic eyes**

Parameter	Cutoff	Sensibility	Especificity	AUROC	IC 95%
p2area	≤1554,438	80.5	96.4	<b>0.939</b>	0,888 to 0,971
p1area	≤2865,500	82.9	89.3	<b>0.929</b>	0,877 to 0,965
p2area1	≤765,625	85.4	90.2	<b>0.926</b>	0,873 to 0,962
h1	≤353,438	80.5	87.5	<b>0.917</b>	0,861 to 0,955
h11	≤235,625	80.5	87.5	<b>0.917</b>	0,861 to 0,955
p1area1	≤1329,750	85.4	85.7	<b>0.908</b>	0,851 to 0,949
CRF	≤8,600	87.8	80.4	<b>0.895</b>	0,835 to 0,939
dive2	≤182,500	68.3	89.3	<b>0.873</b>	0,810 to 0,921
h2	≤266,250	73.2	87.5	<b>0.869</b>	0,805 to 0,918
h21	≤177,500	73.2	87.5	<b>0.869</b>	0,805 to 0,918
CH	≤8,700	75.6	86.6	<b>0.852</b>	0,786 to 0,904
aspect1	≤18,839	87.8	75.0	0.849	0,782 to 0,901
mslew1	≤99,250	82.9	80.4	0.848	0,781 to 0,901
dive1	≤326,500	85.4	75.0	0.845	0,777 to 0,898
uslope1	≤55,700	75.6	81.2	0.840	0,772 to 0,894
IOPg	≤12,100	85.4	77.7	0.830	0,760 to 0,885
dslope1	≤25,841	73.2	79.5	0.814	0,743 to 0,872
slew1	≤62,714	80.5	72.3	0.810	0,739 to 0,869
aspect11	≤23,275	78.0	76.8	0.804	0,732 to 0,864
uslope11	≤48,875	73.2	78.6	0.796	0,723 to 0,857
uslope2	≤46,357	56.1	92.9	0.787	0,713 to 0,849
aplhf	>1,300	87.8	55.4	0.771	0,696 to 0,835
slew2	≤83,833	78.0	66.1	0.768	0,693 to 0,832
mslew2	≤119,000	70.7	73.2	0.761	0,685 to 0,826
aindex	≤8,942	68.3	70.5	0.758	0,682 to 0,824
path2	>27,241	78.0	64.3	0.754	0,678 to 0,820
uslope21	≤46,500	63.4	88.4	0.751	0,675 to 0,817
dslope11	≤31,000	56.1	83.0	0.728	0,650 to 0,796
path1	>25,699	46.3	87.5	0.716	0,638 to 0,786
aspect2	≤17,510	65.9	74.1	0.708	0,629 to 0,779
aspect21	≤21,225	63.4	76.8	0.703	0,624 to 0,774
path21	>43,367	51.2	81.2	0.688	0,609 to 0,761
w21	≤7,000	56.1	72.3	0.682	0,602 to 0,755
path11	≥37,353	51.2	83.0	0.672	0,592 to 0,746
dslope2	≤19,286	53.7	82.1	0.663	0,582 to 0,737
dslope21	≤39,000	68.3	59.8	0.647	0,565 to 0,722
bindex	≤6,290	31.7	96.4	0.644	0,563 to 0,720
w11	≤9,000	43.9	82.1	0.622	0,540 to 0,699
w2	≤13,000	41.5	89.3	0.621	0,540 to 0,698
w1	≤21,000	65.9	53.6	0.586	0,504 to 0,665
IOPcc	≤17,100	90.2	22.3	0.558	0,475 to 0,638

The AUROC was greater than 0.85 for 11 parameters. The parameters related to the area of the waveform during the second and first applanations had the best performances.

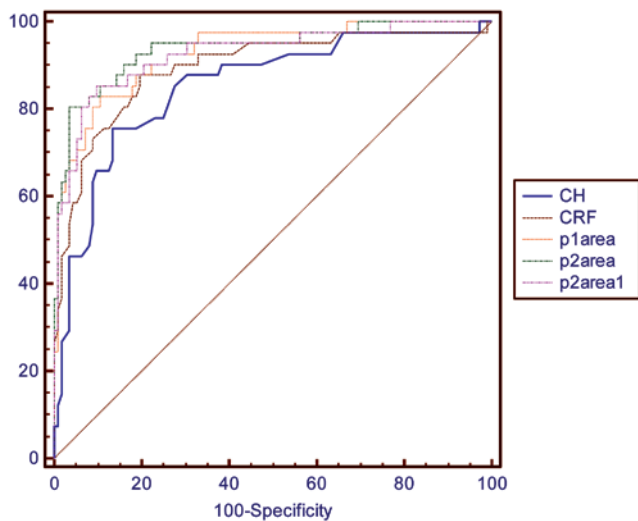
healthy corneas. The AUROCs for p2area and p1area were significantly higher than those for CH and CRF (Table 4). Both p1area and p2area are proportional to the time required to change from the

convex to the concave cornea configuration and vice versa. Small values of p1area and p2area represent rapid change and indicate that the cornea shows less damping<sup>(4)</sup>.

**Table 4. Pairwise comparison of ROC curves**

	P1area	P2area1	H1	H11	P1area1	CRF	Dive2	H2	H21	CH
P2area	0,6914	0,0519	0,4371	0,4371	0,2582	0,1872	0,0340	0,0054	0,0054	0,0181
P1area		0,9011	0,4848	0,4848	0,0228	0,3552	0,0337	0,0142	0,0142	0,0641
P2area1			0,7379	0,7379	0,5084	0,3308	0,0941	0,0250	0,0250	0,0407
H1				1,0000	0,7181	0,5500	0,1158	0,0898	0,0898	0,1388
H11					0,7181	0,5500	0,1158	0,0898	0,0898	0,1388
P1area1						0,7423	0,2463	0,1434	0,1434	0,1984
CRF							0,6450	0,5357	0,5357	0,0161
Dive2								0,8382	0,8382	0,6797
H2									1,0000	0,7185
H21										0,7185

The AUROCs for p2area, p1area, and CRF were significantly greater than the AUROC for CH.



The p2area and p1area were superior to CRF and CH, with AUROCs greater than those for CRF and CH

**Figure 4. Combined receiver operating curves for CH, CRF, P2area, P1area and P2area1.**

The pressure parameters CRF and CH were significant different, as groups, between keratoconus and normal eyes in the present study, with CRF being superior to CH. The importance of CRF compared with CH is consistent with previous findings suggesting that CRF best correlates with optical aberrations in keratoconic eyes<sup>(29)</sup>. However, in the present study, p2area and p1area were superior to CRF and CH, with AUROCs greater than those for CRF and CH (Table 3 and Figure 4). Yet, biomechanical data should not be used as the solo criteria in the diagnosis or screening of keratoconus since corneal curvature (given by Placido disk or corneal tomography elevation technologies) study remains the gold standard.

Further studies are necessary to integrate the parameters derived from the waveform signal with artificial intelligence techniques for detecting corneal curvature characteristics of keratoconus. These sensitive techniques will be useful for detecting milder forms of ectasia when assessing the risk for ectasia after LASIK.

The English in this document has been checked by at least two professional editors, both native speakers of English. For a certificate, please see:

<http://www.textcheck.com/certificate/0eVwb2>

**REFERENCES**

- Luce DA. Determining in vivo biomechanical properties of the cornea with an ocular response analyzer. *J Cataract Refract Surg.* 2005;31(1):156-62.
- Reinstein DZ, Gobbe M, Archer TJ. Ocular biomechanics: measurement parameters and terminology. *J Refract Surg.* 2011;27(6):396-7.
- Spoerl E, Terai N, Scholz F, Raiskup F, Pillunat LE. Detection of biomechanical changes after corneal cross-linking using Ocular Response Analyzer software. *J Refract Surg.* 2011;27(6):452-7.
- Mikielewicz M, Kotliar K, Barraquer RI, Michael R. Air-pulse corneal applanation signal curve parameters for the characterization of keratoconus. *Br J Ophthalmol.* 2011; 95(6):793-8. Comment in: *Br J Ophthalmol.* 2011;95(6):759-60.
- Ambrósio R Jr, Nogueira LP, Caldas DL, Fontes BM, Luz A, Casal JO, et al. Evaluation of corneal shape and biomechanics before LASIK. *Int Ophthalmol Clin.* 2011;51(2):11-38.
- Kerautret J, Colin J, Touboul D, Roberts C. Biomechanical characteristics of the ectatic cornea. *J Cataract Refract Surg.* 2008;34(3):510-3.
- Fry KL, Luce D, Hersh PS. Integrated ocular response analyzer waveform score as a biomechanical index of keratoconus disease severity. In: *Association for Research and Vision in Ophthalmology, 2008; Ft Lauderdale, FL. April 27-May 1.*
- Qazi MA, Sanderson JP, Mahmoud AM, Yoon EY, Roberts CJ, Pepose JS. Postoperative changes in intraocular pressure and corneal biomechanical metrics laser in situ keratomileusis versus laser-assisted subepithelial keratectomy. *J Cataract Refract Surg.* 2009;35(10):1774-88.
- Avetisov SE, Novikov IA, Bubnova IA, Antonov AA, Sipliviy VI. Determination of corneal elasticity coefficient using the ORA database. *J Refract Surg.* 2010;26(7):520-4.
- Sedaghat M, Naderi M, Zarei-Ghanavati M. Biomechanical parameters of the cornea after collagen crosslinking measured by waveform analysis. *J Cataract Refract Surg.* 2010;36(10):1728-31.
- Goldich Y, Barkana Y, Morad Y, Hartstein M, Avni I, Zadok D. Can we measure corneal biomechanical changes after collagen cross-linking in eyes with keratoconus?—a pilot study. *Cornea.* 2009;28(5):498-502.
- Vinciguerra P, Albè E, Mahmoud AM, Trazza S, Hafezi F, Roberts CJ. Intra- and postoperative variation in ocular response analyzer parameters in keratoconic eyes after corneal cross-linking. *J Refract Surg.* 2010;26(9):669-76.
- Fontes BM, Ambrósio R Jr, Velarde GC, Nosé W. Ocular response analyzer measurements in keratoconus with normal central corneal thickness compared with matched normal control eyes. *J Refract Surg.* 2011;27(3):209-15.
- Ortiz D, Piñero D, Shabayek MH, Arnalich-Montiel F, Alió JL. Corneal biomechanical properties in normal, post-laser in situ keratomileusis, and keratoconic eyes. *J Cataract Refract Surg.* 2007;33(8):1371-5. Comment in: *J Cataract Refract Surg.* 2008;34(5): 715; author reply 715-6.
- Shah S, Laiquzzaman M. Comparison of corneal biomechanics in pre and post-refractive surgery and keratoconic eyes by Ocular Response Analyser. *Cont Lens Anterior Eye.* 2009;32(3):129-32; quiz 151.
- Shah S, Laiquzzaman M, Bhojwani R, Mantry S, Cunliffe I. Assessment of the biomechanical properties of the cornea with the ocular response analyzer in normal and keratoconic eyes. *Invest Ophthalmol Vis Sci [Internet].* 2007 [cited 2012 Jun 21]; 48(7): 3026-31. Available from: <http://www.iovs.org/content/48/7/3026> long
- Rabinowitz YS. Keratoconus. *Surv Ophthalmol.* 1998;42(4):297-319.
- Zadnik K, Barr JT, Edrington TB, Everett DF, Jameson M, McMahon TT, et al. Baseline findings in the Collaborative Longitudinal Evaluation of Keratoconus (CLEK) Study. *Invest Ophthalmol Vis Sci [Internet].* 1998 [cited 2011 Jan 2];39(13):2537-46. Available from: <http://www.iovs.org/content/39/13/2537> long
- Luce D. Methodology for cornea compensated IOP and corneal resistance factor for the Reichert Ocular Response Analyzer. *Invest Ophthalmol Vis Sci [Internet].* 2006[ci-

- ted 2012 Jan 21];47:E-Abstract 2266. Available from: <http://abstracts.iovs.org/cgi/content/abstract/47/5/2266?sid=31a0ac4a-7f88-44e0-bcb8-ab9067e023aa>
20. DeLong ER, DeLong DM, Clarke-Pearson DL. Comparing the areas under two or more correlated receiver operating characteristic curves: a nonparametric approach. *Biometrics*. 1988;44(3):837-45.
  21. McNeil BJ, Hanley JA. Statistical approaches to the analysis of receiver operating characteristic (ROC) curves. *Med Decis Making*. 1984;4(2):137-50.
  22. Fontes BM, Ambrósio R Jr, Jardim D, Velarde GC, Nose W. Corneal biomechanical metrics and anterior segment parameters in mild keratoconus. *Ophthalmology*. 2010; 117(4):673-9.
  23. Ambrósio R Jr, Caiado AL, Guerra FP, Louzada R, Roy AS, Luz A, et al. Novel pachymetric parameters based on corneal tomography for diagnosing keratoconus. *Refract Surg*. 2011;27(10):753-8.
  24. Krachmer JH, Feder RS, Belin MW. Keratoconus and related noninflammatory corneal thinning disorders. *Surv Ophthalmol*. 1984;28(4):293-322.
  25. Sawaguchi S, Yue B, Chang I, Sugar J, Robin J. Proteoglycan molecules in keratoconus corneas. *Invest Ophthalmol Vis Sci* [Internet]. 1991[cited 2011 Jun 21];32(6):1846-53. Available from: <http://www.iovs.org/content/32/6/1846.long>
  26. Mackiewicz Z, Maatta M, Stenman M, Konttinen L, Tervo T, Konttinen YT. Collagenolytic proteinases in keratoconus. *Cornea*. 2006;25(5):603-10. Erratum In: *Cornea*. 2006; 25(6):760.
  27. Reeves SW, Ellwein LB, Kim T, Constantine R, Lee PP. Keratoconus in the Medicare population. *Cornea*. 2009;28(1):40-2.
  28. Saad A, Lteif Y, Azan E, Gatineau D. Biomechanical properties of keratoconus suspect eyes. *Invest Ophthalmol Vis Sci* [Internet]. 2010[cited 2012 Mar 21];51(6):2912-6. Available from: <http://www.iovs.org/content/51/6/2912.long>
  29. Piñero DP, Alió JL, Barraquer RI, Michael R, Jiménez R. Corneal biomechanics, refraction, and corneal aberrometry in keratoconus: an integrated study. *Invest Ophthalmol Vis Sci* [Internet]. 2010[cited 2012 Nov 21];51(4):1948-55. Available from: <http://www.iovs.org/content/51/4/1948.long>

## XXXVII Congresso Brasileiro de Oftalmologia

## XXX Congresso Pan-Americano de Oftalmologia

7 a 10 de agosto de 2013

RioCentro  
Rio de Janeiro (RJ)

**Informações:**  
Site: [www.cbo2013.com.br](http://www.cbo2013.com.br)